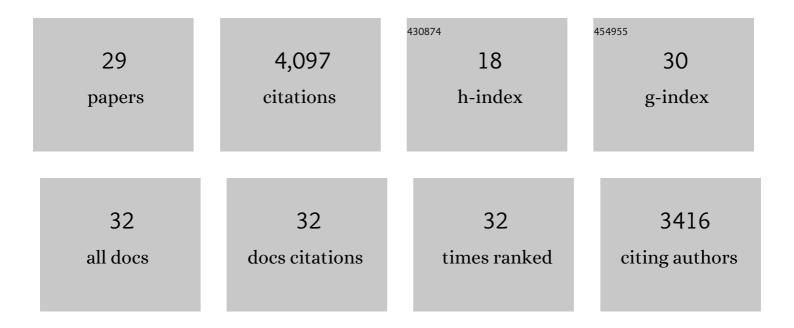
Tim Holland-Letz

List of Publications by Year in descending order

Source: https://exaly.com/author-pdf/7347635/publications.pdf Version: 2024-02-01



#	Article	IF	CITATIONS
1	An R-shiny application to calculate optimal designs for single substance and interaction trials in dose response experiments. Toxicology Letters, 2021, 337, 18-27.	0.8	2
2	Diagnostic Accuracy of ¹⁸ F-PSMA-1007 PET/CT Imaging for Lymph Node Staging of Prostate Carcinoma in Primary and Biochemical Recurrence. Journal of Nuclear Medicine, 2021, 62, 208-213.	5.0	77
3	Performance of [68Ga]Ga-PSMA-11 PET/CT in patients with recurrent prostate cancer after prostatectomy—a multi-centre evaluation of 2533 patients. European Journal of Nuclear Medicine and Molecular Imaging, 2021, 48, 2925-2934.	6.4	43
4	Predicting the Risk of Metastases by PSMA-PET/CT—Evaluation of 335 Men with Treatment-NaÃ⁻ve Prostate Carcinoma. Cancers, 2021, 13, 1508.	3.7	8
5	68Ga-PSMA-11 PET/CT in patients with recurrent prostate cancer—a modified protocol compared with the common protocol. European Journal of Nuclear Medicine and Molecular Imaging, 2020, 47, 624-631.	6.4	26
6	Modeling dose–response functions for combination treatments with log-logistic or Weibull functions. Archives of Toxicology, 2020, 94, 197-204.	4.2	4
7	The design heatmap: A simple visualization of â€optimality design problems. Biometrical Journal, 2020, 62, 2013-2031.	1.0	1
8	Drawing statistical conclusions from experiments with multiple quantitative measurements per subject. Radiotherapy and Oncology, 2020, 152, 30-33.	0.6	1
9	⁶⁸ Ga-PSMA-11 PET/CT in Primary and Recurrent Prostate Carcinoma: Implications for Radiotherapeutic Management in 121 Patients. Journal of Nuclear Medicine, 2019, 60, 234-240.	5.0	49
10	Comparison of PSMA-ligand PET/CT and multiparametric MRI for the detection of recurrent prostate cancer in the pelvis. European Journal of Nuclear Medicine and Molecular Imaging, 2019, 46, 2289-2297.	6.4	19
11	Tracer uptake in mediastinal and paraaortal thoracic lymph nodes as a potential pitfall in image interpretation of PSMA ligand PET/CT. European Journal of Nuclear Medicine and Molecular Imaging, 2018, 45, 1179-1187.	6.4	26
12	Intraindividual Comparison of ^{99m} Tc-Methylene Diphosphonate and Prostate-Specific Membrane Antigen Ligand ^{99m} Tc-MIP-1427 in Patients with Osseous Metastasized Prostate Cancer. Journal of Nuclear Medicine, 2018, 59, 1373-1379.	5.0	31
13	Optimal experimental designs for estimating the drug combination index in toxicology. Computational Statistics and Data Analysis, 2018, 117, 182-193.	1.2	7
14	Impact of long-term androgen deprivation therapy on PSMA ligand PET/CT in patients with castration-sensitive prostate cancer. European Journal of Nuclear Medicine and Molecular Imaging, 2018, 45, 2045-2054.	6.4	116
15	Parametric modeling and optimal experimental designs for estimating isobolograms for drug interactions in toxicology. Journal of Biopharmaceutical Statistics, 2018, 28, 763-777.	0.8	4
16	On the Combination of <i>c</i> - and <i>D</i> -Optimal Designs: General Approaches and Applications in Dose–Response Studies. Biometrics, 2017, 73, 206-213.	1.4	7
17	The Clinical Impact of Additional Late PET/CT Imaging with ⁶⁸ Ga-PSMA-11 (HBED-CC) in the Diagnosis of Prostate Cancer. Journal of Nuclear Medicine, 2017, 58, 750-755.	5.0	105
18	Repeated PSMA-targeting radioligand therapy of metastatic prostate cancer with 131I-MIP-1095. European Journal of Nuclear Medicine and Molecular Imaging, 2017, 44, 950-959.	6.4	69

#	Article	IF	CITATIONS
19	Diagnostic performance of 68Ga-PSMA-11 (HBED-CC) PET/CT in patients with recurrent prostate cancer: evaluation in 1007 patients. European Journal of Nuclear Medicine and Molecular Imaging, 2017, 44, 1258-1268.	6.4	425
20	Intraindividual Comparison of ¹⁸ F-PSMA-1007 PET/CT, Multiparametric MRI, and Radical Prostatectomy Specimens in Patients with Primary Prostate Cancer: A Retrospective, Proof-of-Concept Study. Journal of Nuclear Medicine, 2017, 58, 1805-1810.	5.0	91
21	⁶⁸ Ga-PSMA PET/CT and Volumetric Morphology of PET-Positive Lymph Nodes Stratified by Tumor Differentiation of Prostate Cancer. Journal of Nuclear Medicine, 2017, 58, 1949-1955.	5.0	27
22	Intra-individual comparison of 68Ga-PSMA-11-PET/CT and multi-parametric MR for imaging of primary prostate cancer. European Journal of Nuclear Medicine and Molecular Imaging, 2016, 43, 1400-1406.	6.4	101
23	Optimal experimental designs for dose–response studies with continuous endpoints. Archives of Toxicology, 2015, 89, 2059-2068.	4.2	29
24	The Theranostic PSMA Ligand PSMA-617 in the Diagnosis of Prostate Cancer by PET/CT: Biodistribution in Humans, Radiation Dosimetry, and First Evaluation of Tumor Lesions. Journal of Nuclear Medicine, 2015, 56, 1697-1705.	5.0	332
25	The diagnostic value of PET/CT imaging with the 68Ga-labelled PSMA ligand HBED-CC in the diagnosis of recurrent prostate cancer. European Journal of Nuclear Medicine and Molecular Imaging, 2015, 42, 197-209.	6.4	866
26	Comparison of PET imaging with a 68Ga-labelled PSMA ligand and 18F-choline-based PET/CT for the diagnosis of recurrent prostate cancer. European Journal of Nuclear Medicine and Molecular Imaging, 2014, 41, 11-20.	6.4	817
27	Reply to Reske et al.: PET imaging with a [68Ga]gallium-labelled PSMA ligand for the diagnosis of prostate cancer: biodistribution in humans and first evaluation of tumour lesions. European Journal of Nuclear Medicine and Molecular Imaging, 2013, 40, 971-972.	6.4	20
28	PET imaging with a [68Ga]gallium-labelled PSMA ligand for the diagnosis of prostate cancer: biodistribution in humans and first evaluation of tumour lesions. European Journal of Nuclear Medicine and Molecular Imaging, 2013, 40, 486-495.	6.4	773
29	Efficient Algorithms for Optimal Designs with Correlated Observations in Pharmacokinetics and Doseâ€Finding Studies. Biometrics, 2012, 68, 138-145.	1.4	6